RAPID COMMUNICATIONS

PHYSICAL REVIEW C VOLUME 51, NUMBER 2 FEBRUARY 1995

Superdeformation in ^{193}Pb and the effects of the $N=7$ intruder orbital

J. R. Hughes, J. A. Becker, L. A. Bernstein, M. J. Brinkman,* L. P. Farris, E. A. Henry, R. W. Hoff, M. A. Stoyer,† and D. T. Vo
Lawrence Livermore National Laboratory, Livermore, California 94550

S. Asztalos, B. Cederwall, R. M. Clark, M. A. Deleplanque, R. M. Diamond, P. Fallon, I. Y. Lee, A. O. Macchiavelli, and F. S. Stephens
Lawrence Berkeley Laboratory, Berkeley, California 94720

(Received 21 October 1994)

Six superdeformed bands have been observed in ^{193}Pb following the ^{174}Yb(^{24}Mg,5n) reaction at a beam energy of 131 MeV. The in-beam γ rays were detected with GAMMASPHERE early implementation. Two of the bands have dynamic moments of inertia which have an anomalously low increase with rotational frequency, and are interpreted as the favored and unfavored signature components of the $N=7$ neutron orbital. The other four bands have increasing dynamic moments of inertia typical of superdeformed bands in the $A=190$ region, and are interpreted as two pairs of signature partner bands based on high-K quasineutron excitations. The effects of the intruder $N=7$ neutron orbital on the superdeformed rotational characteristics are discussed.

PACS number(s): 21.10.Re, 21.60.Ev, 27.80.+w

Superdeformation is now well established in a number of mass regions throughout the Segré chart (see Ref. [1], and references therein). In the $A=190$ region over 40 superdeformed (SD) bands have been observed in 16 nuclei. In contrast to SD nuclei in the $A=150$ region, whose dynamic moments of inertia ($\mathscr{J}^{(2)}$) show a variety of behaviors as a function of rotational frequency ($\hbar\omega$), the majority of the SD bands in the $A=190$ region have a $\mathscr{J}^{(2)}$ with a very similar $\hbar\omega$ dependence. These qualitatively different systematics may be related to the different ranges of angular momentum at which SD bands in the different mass regions exist. Pairing correlations are expected to be negligible for $A=150$ SD nuclei due to the large amount of angular momentum, and the $\mathscr{J}^{(2)}$ are successfully interpreted in terms of high-N orbital occupations [2]. For $A=190$ SD nuclei, however, which occur at lower values of angular momentum, pairing correlations are expected to be more important. The $\mathscr{J}^{(2)}$ of most $A=190$ SD nuclei are characterized by a smooth increase with increasing $\hbar\omega$. This rise has been interpreted as being due to the combined alignment of both high-N quasiprotons and quasineutrons and a corresponding reduction in the pairing [3,4].

Experimental confirmation of this scenario is limited. Two SD bands in the odd-odd ^{192}Tl nucleus have been observed where the $\mathscr{J}^{(2)}$ does not display the typical rise with increasing $\hbar\omega$ [5]. Liang *et al.* suggest that the Pauli blocking of both intruder quasiproton and quasineutron alignments (double-blocking) is responsible for the reduced $\mathscr{J}^{(2)}$ slope observed in these bands. In addition, the reduction in pairing and the contribution of the single-particle alignments result in a slightly higher $\mathscr{J}^{(2)}$ at lower $\hbar\omega$. These features are qualitatively in accordance with our understanding of pairing and alignment processes. A similar interpretation in the only other known odd-odd SD nucleus in this region, ^{194}Tl [6], seems possible, although all the known SD bands show at least some increase of $\mathscr{J}^{(2)}$ with $\hbar\omega$. Other examples of SD bands which show a relatively flat $\mathscr{J}^{(2)}$ over some frequency range have been interpreted as evidence for a level crossing [7] and occupation of the unfavored $N=7$ neutron orbital [8].

The recent observation of two SD bands in ^{195}Pb [9] with essentially constant $\mathscr{J}^{(2)}$, however, poses questions for our understanding of the pairing correlations and alignment processes in SD nuclei in this region. These "flat bands," being the most intensely populated SD bands in this nucleus, presumably contain no quasiproton excitations, and so double-blocking cannot be invoked as an explanation for the flat $\mathscr{J}^{(2)}$. Farris *et al.* [9] suggested that the flat $\mathscr{J}^{(2)}$ of these bands may be due to the blocked quasineutron alignment coupled to a reduced, or delayed quasiproton alignment. In this Rapid Communication we present evidence for six superdeformed bands in ^{193}Pb, two of which have moments of inertia which are flat with respect to $\hbar\omega$. This observation suggests that the flat bands in the odd Pb nuclei may be a systematic effect, related to changes in the pairing correlations, deformation, or Fermi surface.

The ^{193}Pb data set was obtained using the ^{174}Yb(^{24}Mg, 5n) reaction at a beam energy of 131 MeV. The target consisted of a stack of three self-supporting thin foils, each $\sim$500 μg/cm^2. The beam was provided by the 88-Inch Cyclotron Facility, and γ-ray spectroscopy was done with GAMMASPHERE early implementation. Thirty-six Compton-suppressed Ge detectors were in place for this experiment, six at 90°, and 15 each at backward and forward angles with respect to the beam axis. The data set comprised approximately 5×10^8 three- and higher-fold events, yielding 9×10^8 expanded threefold events. These events were sorted into a symmetrized three-dimensional cube with 900 channels on each axis. Gated twofold asymmetric matrices have

*Present address: Oak Ridge National Laboratory, Oak Ridge, TN 37831.

†Present address: Lawrence Berkeley Laboratory, Berkeley, CA 94720.

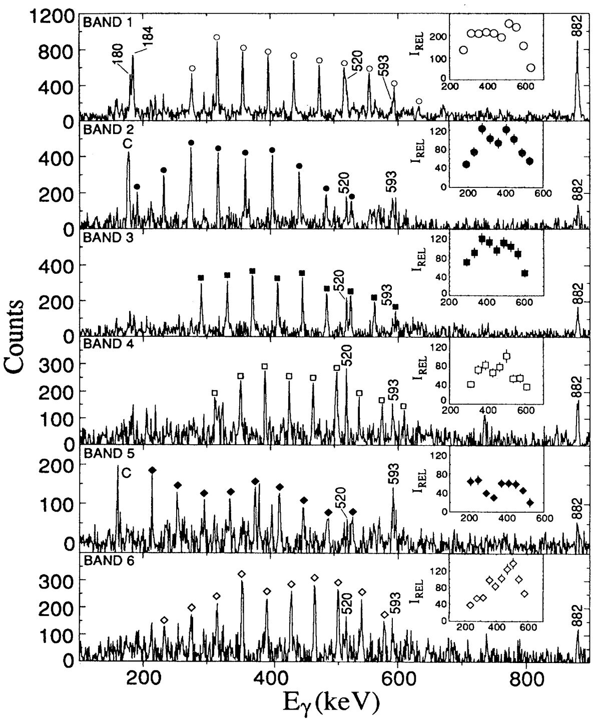

FIG. 1. Background-subtracted spectra for the six SD bands observed in ^{193}Pb. Band members are denoted by ○–band 1, ●–band 2, ■–band 3, □–band 4, ◆–band 5, and ◇–band 6. (See Table I for transition energies.) Low-lying yrast transitions are labeled by energy in keV, and known contaminant lines by "C." The relative intensity of each band is shown inset.

been produced for events with γ rays detected at forward/backward, and 90° angles. Such matrices were made with gates on normal yrast lines, and gates on each of the six SD bands. In addition, a full-resolution two-dimensional matrix (4096 channels), has been sorted from the expanded doubles events. The data have been searched for SD bands with standard γ-ray spectroscopic methods, and an automated computer algorithm [10].

Double-gated background-subtracted spectra for the six new SD bands found in these data are presented in Fig. 1 (see also Table I). The relative intensities of the ^{193}Pb SD bands are shown in the inset of Fig. 1. The estimated intensity of each band relative to the total ^{193}Pb channel is 0.5, 0.3, 0.25, 0.25, 0.2, and 0.2%, respectively. These new bands are assigned to ^{193}Pb based on cross bombardment and coincidence information. All the bands are in coincidence with known transitions in ^{193}Pb [11]. There is evidence for the 593.1-, 520.2-, and 881.6-keV transitions between the low-lying positive-parity states in coincidence with each of the bands. In addition, the coincidence relationships suggest that band 1 also feeds the $23/2^-$ state (180- and 184-keV transitions). The cross-bombardment information also supports the assignment of all six bands to ^{193}Pb. The $4n(^{194}$Pb) channel is present in this data, and the ^{194}Pb(1) SD band is observed, but no evidence for the six new SD bands can be found in the comparable ^{194}Pb data set [12]. In addition, no evidence for the known SD band in ^{192}Pb [13] can be found in the present data. This suggests that the new SD bands are not associated with either ^{192}Pb or ^{194}Pb. The predominant charged-particle evaporation channels are $\alpha 4n(^{190}$Hg) and $p4n(^{193}$Tl), but represent only ~ 10% and 5%, respectively, of the $5n$ channel yield. If the observed SD bands were associated with either of these charged particle channels, they would represent ~ 5% and 10% of the respective channel yield. These yields would be unrealistic since they are already greater than the observed yields of the strongest known SD bands in these nuclei.

The angle asymmetric matrices have been used to determine angular asymmetries for transitions in ^{193}Pb. Bernstein *et al.* [14] have shown that γ-ray asymmetry ratios for known stretched quadrupole and stretched dipole transitions are distinguishable with the present detector geometry. Averaged normalized ratios of γ-ray intensities at forward/backward angles to those at 90° are found to be 1.00(5) for known stretched $E2$, and 0.40(3) for known stretched $M1$ transitions in ^{193}Pb. The asymmetry ratios for 11 transitions in five of the ^{193}Pb SD bands have been determined, and are more consistent with those expected for stretched quadrupole rather than stretched dipole. We make the reasonable assumption that these transitions are of $E2$ character.

A number of features are readily apparent in the spectra of Fig. 1. The transition energies of ^{193}Pb(4) are midway between those of ^{193}Pb(3) over the frequency range observed. This feature suggests that these bands are a pair of signature partners (with no signature splitting) based on a high-K orbital. A similar relationship is apparent for the pair ^{193}Pb(5,6). The bands ^{193}Pb(1,2), however, do not show this

TABLE I. Transitions energies of the six new bands observed in ^{193}Pb.

Band 1	Band 2	Band 3	Band 4	Band 5	Band 6
276.63(28)	190.54(20)	291.57(31)	313.84(32)	213.27(29)	232.86(19)
317.33(32)	232.14(19)	332.28(30)	353.35(34)	254.71(23)	275.70(21)
357.27(31)	275.46(21)	372.42(26)	391.99(45)	295.13(21)	316.79(18)
397.28(30)	318.15(23)	412.04(35)	430.13(35)	335.70(24)	356.42(13)
437.63(35)	360.69(23)	450.62(50)	467.22(28)	375.04(24)	394.48(19)
477.52(55)	403.66(34)	488.69(110)	503.97(67)	413.81(16)	432.94(19)
516.92(52)	445.99(31)	525.98(95)	539.51(88)	451.27(50)	470.27(21)
555.84(60)	488.12(114)	563.57(120)	575.30(65)	489.01(54)	507.13(25)
593.75(70)	527.51(74)	599.90(120)	609.56(73)	527.00(100)	543.57(46)
632.46(100)					579.25(36)

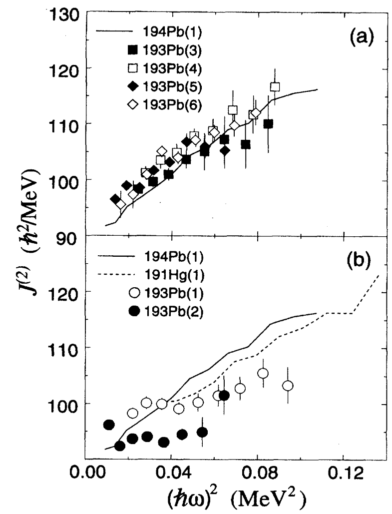

FIG. 2. $\mathscr{J}^{(2)}$ vs $(\hbar\omega)^2$ for the six SD bands in ^{193}Pb. The same symbols as in Fig. 1 are used for each band.

behavior. We suggest that they are a pair of signature-split bands based on the favored and unfavored signature components of the low-K $N=7$ neutron orbital. These interpretations are based on the observed $\mathscr{J}^{(2)}$ and Routhians, e', and are compared to cranked shell model (CSM) calculations and neighboring SD nuclei in the following sections.

We have performed cranked-shell-model (CSM) calculations [15] to examine the quasineutron orbitals near the $N=111$ Fermi surface. These calculations were performed at a deformation $\beta_2=0.478$, $\beta_4=0.07$, and $\gamma=0°$. Total-Routhian-surface calculations [16] indicate that this is a representative deformation for SD bands in ^{193}Pb, although small differences in deformation for different configurations are predicted. The pairing interaction was of the monopole type, with an initial value $\Delta=0.7$ MeV at $\hbar\omega=0$ MeV, and a parametrized reduction with increasing $\hbar\omega$ [15]. The CSM calculations are in qualitative agreement with recent Hartree-Fock-Bogoliubov (HFB) calculations [17], with very similar low-lying excitations at $\hbar\omega=0$ MeV. It should be noted, however, that the HFB calculations referred to above are more appropriate for the Hg than the Pb nuclei—the associated differences in calculated deformation may explain the small differences in level energies between the HFB and CSM results. Nevertheless, both the HFB and CSM calculations predict that the lowest lying high-K quasineutron excitations should be based on the [624]9/2 and [512]5/2 orbitals. In addition, the $N=7$ neutron orbital (predominantly $\Omega=3/2$) is calculated to be a low-lying excitation, which is strongly favored by rotation.

The $\mathscr{J}^{(2)}$ versus the square of rotational frequency, $\hbar\omega$, for the six SD bands in ^{193}Pb and that in ^{194}Pb(1) [22], and ^{191}Hg [18] are shown in Figs. 2(a) and 2(b). Bands ^{193}Pb(3,4), and ^{193}Pb(5,6) [Fig. 2(a)] display the typical rise in $\mathscr{J}^{(2)}$ with increasing $\hbar\omega$, as has been observed in most other SD bands in this region, and are very similar to that in ^{194}Pb(1). The rise in the $\mathscr{J}^{(2)}$ is thought to be due to the sequential alignment of $N=7$ quasineutrons, and $N=6$ quasiprotons [3,4]. Bands ^{193}Pb(1,2) [Fig. 2(b)], however, have a much reduced $\mathscr{J}^{(2)}$ slope with increasing $\hbar\omega$. In the frequency range that ^{193}Pb(1,2) are observed, the alignment of $N=7$ quasineutrons is expected to dominate the contribution to the rise in $\mathscr{J}^{(2)}$. The absence of such a rise for ^{193}Pb(1,2) implies that the quasineutron alignment is blocked, consistent with the interpretation that ^{193}Pb(1,2) are based on the favored and unfavored signature components of the $N=7$ neutron orbital, respectively. In addition, ^{193}Pb(1) has a larger average $\mathscr{J}^{(2)}$ value than that for ^{193}Pb(2). A similar relationship has been observed for the $N=7$ signature-partner bands in both ^{193}Hg [8] and ^{195}Pb [9].

The $\hbar\omega$ dependence of the $\mathscr{J}^{(2)}$ of the favored $N=7$ band [^{193}Pb(1)], however, is in striking variance to similar bands in the odd-Hg nuclei (^{189}Hg [4] and ^{191}Hg [19]) which generally show a substantial increase in $\mathscr{J}^{(2)}$ with increasing $\hbar\omega$. In particular, the SD band assigned to the favored $N=7$ neutron orbital in the $N=111$ isotone, ^{191}Hg(1), shown in Fig. 2(b), has a much larger $\mathscr{J}^{(2)}$ slope than that of ^{193}Pb(1). Indeed, ^{191}Hg(1) has a $\mathscr{J}^{(2)}$ increase which is comparable to that observed in the two excited SD bands in this nucleus [19]. The $\mathscr{J}^{(2)}$ of ^{195}Pb(1,2) are also essentially flat with increasing $\hbar\omega$, in addition to those of ^{193}Pb(1,2). This, coupled to the observations in odd-Hg nuclei, suggests that there is a systematic difference in the behavior of the $\mathscr{J}^{(2)}$ in Pb and Hg SD nuclei, when the $N=7$ quasineutron alignment is blocked.

These differences may be related to the behavior of the $N=7$ orbital as a function of deformation, pairing, or Fermi surface changes. The contribution of an individual orbital to the $\mathscr{J}^{(2)}$ can be related to the second derivative of the Routhian, e', with respect to the rotational frequency, ω, $\Delta\mathscr{J}^{(2)}=-d^2e'/d\omega^2=di/d\omega$, where i is the alignment. The large positive curvature of the unfavored $N=7$ orbital [around $\hbar\omega=0.2$ MeV, see Fig. 3(b)], for instance, probably explains why the bands associated with it have a smaller average $\mathscr{J}^{(2)}$ than bands based on the favored component. Other orbitals near the Fermi surface with little or no dependence on $\hbar\omega$, on the other hand, should have little effect on $\mathscr{J}^{(2)}$. CSM calculations specific to ^{193}Pb and ^{191}Hg, confirm that bands associated with the unfavored $N=7$ neutron orbital should have a smaller $\mathscr{J}^{(2)}$ than that associated with the favored component; the difference is calculated to be $\sim$ 10 $\hbar^2$/MeV. In addition, the specific curvature of these orbitals may have an appreciable effect on $\mathscr{J}^{(2)}$. It is difficult, however, to explain the differences observed between ^{193}Pb and ^{191}Hg with this mechanism. Although the small differences in deformation between ^{193}Pb and ^{191}Hg SD nuclei have a noticeable effect on the single-particle energies (and hence e' at $\hbar\omega=0$ MeV), no appreciable difference in i, or $di/d\omega$ of the $N=7$ orbital is apparent. Differences in neutron pairing, and changes in the neutron Fermi surface (which strongly affect interaction strengths) however, may substantially affect i and $di/d\omega$.

Another possible cause for the different $\mathscr{J}^{(2)}$ behavior is that the quasiproton alignment is quenched in Pb nuclei, compared to that in Hg nuclei. Indeed, a reduction in the quasiproton alignment is qualitatively expected in the Pb nuclei with respect to the Hg nuclei for two related reasons. First, an increase in the proton Fermi surface energy by the addition of two protons, and second a slight increase in the

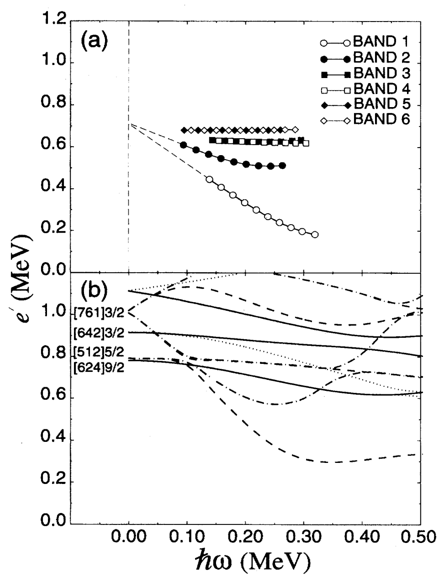

FIG. 3. (a) Experimental Routhians for the six SD bands observed in ^{193}Pb. The relative excitation energy of each band is unknown: the bands are plotted such that bands interpreted as signature partners extrapolate to the same value of e' at $\hbar\omega=0$. (b) Calculated quasineutron Routhians (see text for details). Orbitals are labeled at $\hbar\omega$ with the predominant Nilsson component.

deformation both serve to increase the excitation energy of the lower-Ω components of the $N=6$ proton intruder orbital, and move higher-Ω components closer to the Fermi surface. This has the effect of increasing the quasiproton alignment frequency in Pb nuclei. The rising $\mathscr{J}^{(2)}$ for ^{193}Pb(3,4) and ^{193}Pb(5,6) may then be explained as predominantly due to quasineutron alignment, whereas the flat $\mathscr{J}^{(2)}$ for ^{193}Pb(1,2) is a result of blocking the quasineutron alignment. In the Hg nuclei, a substantially lower quasiproton alignment frequency results in a rising $\mathscr{J}^{(2)}$ even for quasineutron blocked bands, as suggested by Carpenter *et al.* [19] for ^{191}Hg(1). Although this may explain the $\mathscr{J}^{(2)}$ differences between odd-neutron Pb and Hg SD nuclei, the similarity between the $\mathscr{J}^{(2)}$ of the even-even Pb and Hg nuclei (particularly ^{194}Pb and ^{192}Hg) in the presence of changes in pairing and deformation is remarkable. As alluded to above, however, the $\mathscr{J}^{(2)}$ is sensitive to a number of quantities. A systematic description of the $\mathscr{J}^{(2)}$ throughout the $A=190$ region will require a detailed understanding of the pairing correlations, possibly including higher multipoles in the pairing field, and/or a residual neutron-proton interaction. These types of calculations are beyond the scope of this Rapid Communication, but we believe that the specific mechanisms mentioned above probably play an important role in the behavior of the $\mathscr{J}^{(2)}$.

In order to further compare with theory, we have transformed the experimental data into the rotating frame of reference using the prescription described in Ref. [20]. To achieve this transformation, a knowledge of the level spins is required. We have estimated the level spins for ^{193}Pb(3,4) and ^{193}Pb(5,6) using the method of Becker *et al.* [21]. The extracted spin of the lowest level in each band, I_f, and the χ^2 per degree of freedom [χ^2/ν] are 12.3(2) [0.13], 13.7(2) [0.18], 8.5(1) [0.71], 9.4(1) [3.2], respectively. We have chosen not to use fitted spin values for ^{193}Pb(1,2). These bands are probably based on the low-Ω $N=7$ neutron orbital, which may exhibit considerable alignment at low $\hbar\omega$ (see CSM calculations). Such behavior may induce variations in the $\mathscr{J}^{(2)}$ in the frequency range below that which these bands are observed. As suggested in Ref. [21] the spin fit method is probably not appropriate for these types of bands, as was already noted for ^{189,191}Hg(1). For the following discussion we will adopt $I_f=27/2$ [^{193}Pb(1)], and $I_f=17/2$ [^{193}Pb(2)]. These values are primarily chosen based on the feeding of the normal states, but also represent the nearest half-integer value of the correct signature to that provided by the spin fit method.

The experimental Routhians, e', for the six bands are shown in Fig. 3(a). The Routhians have been extracted using the Harris parameters $J_0=92.7\hbar^2/\mathrm{MeV}$, $J_1=97.6\hbar^4/\mathrm{MeV}^3$, which were chosen to yield a flat e' for ^{193}Pb(5,6). The spin values used are the closest half-integer to the fitted spins (quoted above), and the K-values are 3/2 [^{193}Pb(1,2)], 5/2 [^{193}Pb(3,4)], and 9/2 [^{193}Pb(5,6)]. The relative excitation energies of the six bands are unknown, and thus the e' are on a floating energy scale. Bands interpreted as signature partners, however, are plotted such that the e' extrapolate to the same value at $\hbar\omega=0$ MeV. It is clear that ^{193}Pb(1,2) are strongly favored with increasing $\hbar\omega$ relative to the other four bands. This observation is in agreement with CSM calculations which predict that the $N=7$ orbital has substantially more alignment than the other orbitals near the neutron Fermi surface. Assuming the relative excitation energy of ^{193}Pb(1,2) is given by the abovementioned condition, we extract a signature splitting of ~ 200 keV at $\hbar\omega=0.2$ MeV. The CSM results shown in Fig. 3(b) predict that this orbital has a signature splitting of ~ 130 keV at $\hbar\omega=$ 0.2 MeV. The only other low-lying orbital calculated to have appreciable signature splitting is the [642]3/2, with $\Delta e' \sim 30$ keV at $\hbar\omega=$ 0.2 MeV (this is very close to the experimentally estimated value in ^{191}Hg [19]). The $N=7$ orbital, however, is calculated to be much more favored by rotation, with an alignment of ~ 2.5 $\hbar$ for the favored signature, compared to that of ~ 0.8 $\hbar$ for the [642]3/2 orbital. The experimental value extracted for ^{193}Pb(1) is ~ 1.9 $\hbar$, although it should be noted that this value is quite sensitive to the assumed spin values. However, we do not observe a SD band(s) with characteristics consistent with the [642]3/2 orbital, even though it is calculated to be a relatively low-lying excitation.

Another interesting feature apparent in the calculations is the interaction between the $N=7$ and 5 orbitals. The first interaction takes place at $\hbar\omega \approx 0.10$ MeV where both signatures of the $N=7$ orbital cross those of the $N=5$ orbital. A second interaction also takes place at a higher frequency, $\hbar\omega \approx 0.35$ MeV, when the unfavored component of the $N=7$ orbital interact with the same signature of the $N=5$ orbital. In the case of ^{193}Hg an interaction is clearly visible in the data, allowing an experimental estimate of both the interaction strength, and the relative energies of the $N=$ 7 and 5 orbitals [7]. No such clear interaction is present in ^{193}Pb. This is most likely due to the neutron Fermi surface being relatively lower in ^{193}Pb than ^{193}Hg, effectively lowering the energy of the low-Ω $N=7$ orbital, and reducing the frequency at which it crosses the $N=5$ orbital. However, a close inspection of the experimental Routhians reveals that ^{193}Pb(3) shows an upturn relative to ^{193}Pb(4) at the highest frequencies, where the unfavored component of the $N=7$ band [^{193}Pb(2)] begins to come close in energy. This may indicate a band interaction, which requires that ^{193}Pb(1,2) and ^{193}Pb(3,4) have the same parity, and further that ^{193}Pb(2) and ^{193}Pb(3) have the same signature. Thus ^{193}Pb(3,4) may be associated with the $N=5$ high-K orbital, although this assignment is tentative.

One possible way to distinguish between bands based on the [624]9/2 and [512]5/2 neutron orbitals is to measure the $B(M1)/B(E2)$ branching ratios. This method has been applied to SD bands in ^{193}Hg [23], where good agreement between the estimated and predicted g_K-value for the [512]5/2 configuration was obtained. We have examined the ^{193}Pb SD bands for evidence of cross-talk. No γ-transitions between pairs of bands have been observed for any of the bands, but it appears from Fig. 1 that bands 5 and 6 are in mutual coincidence at lower frequencies. It should be noted that the relative intensity of this cross-talk is rather sensitive to the gating conditions and the background subtraction. We estimate, however, that $B(M1)/B(E2)\sim 0.05(3)$ for bands 5 and 6. For bands 3 and 4, the lack of observed cross-talk implies an upper limit of $B(M1)/B(E2)=0.03$. Unfortunately, this degree of accuracy is not sufficient to unambiguously distinguish between the two possible neutron orbitals.

In conclusion, we have identified six superdeformed bands in ^{193}Pb. Four of the bands form two pairs of signature partners based on high-K neutron orbitals. The most likely orbitals to be involved are the [624]9/2 and [512]5/2 neutron orbitals. A perturbation to the Routhian of band 3 suggests that ^{193}Pb(3,4) may be based on the [512]5/2 neutron orbital, although this assignment is tentative. The other two bands are proposed to be based on the favored and unfavored signature components of the $N=7$ neutron orbital. The estimated alignment and signature splitting are in qualitative agreement with CSM calculations. These bands have a flat $\mathscr{J}^{(2)}$ with respect to $\hbar\omega$, which is in striking variance to similar bands in odd-Hg nuclei. We propose that this difference is due either to the Pauli blocking of the $N=7$ orbital coupled to a quenching of the quasiproton pair-alignment contribution, or to the specific curvature of the orbitals involved.

We would like to thank D. C. Radford for use of his analysis codes. We thank the 88-Inch Cyclotron crew for flawless operation. Joanne Heagney of Micromatter made the targets. This work was supported in part by the U.S. Department of Energy, under Contract No. W7405-ENG-48 (LLNL), and No. DE-AC03-76SF00098 (LBL).

[1] R. B. Firestone and B. Singh, "Table of Superdeformed Nuclear Bands," LBL Report No. LBL-35916 (unpublished).
[2] T. Bengtsson, I. Ragnarsson, and S. Aberg, Phys. Lett. B **208**, 39 (1988); W. Nazarewicz, R. Wyss, and A. Johnson, Nucl. Phys. **A503**, 285 (1989).
[3] M. A. Riley *et al.*, Nucl. Phys. **A512**, 178 (1990).
[4] M. W. Drigert *et al.*, Nucl. Phys. **A530**, 452 (1991).
[5] Y. Liang *et al.*, Phys. Rev. C **46**, R2136 (1992).
[6] F. Azaiez *et al.*, Phys. Rev. Lett. **66**, 1030 (1991).
[7] D. M. Cullen *et al.*, Phys. Rev. Lett. **65**, 1547 (1990).
[8] M. J. Joyce *et al.*, Phys. Lett. B **340**, 150 (1994).
[9] L. P. Farris *et al.* (unpublished); E. A. Henry *et al.*, Bull. Am. Phys. Soc. **39**, 1184 (1994).
[10] J. R. Hughes *et al.* (unpublished).
[11] M. A. Stoyer *et al.*, Proceedings of the 205th ACS meeting, Denver Colorado, 1993, Part II, Abstract number NUCL-56 (unpublished); M. A. Stoyer *et al.* (unpublished).
[12] M. J. Brinkman *et al.* (unpublished).
[13] E. A. Henry *et al.*, Z. Phys. A **338**, 469 (1991).
[14] L. A. Bernstein *et al.* (unpublished).
[15] R. Wyss, Nuclear Structure Theory Workshop, Oak Ridge, Tennessee, 1991 (unpublished).
[16] R. Wyss, W. Satula, W. Nazarewicz, and A. Johnson, Nucl. Phys. **A511**, 324 (1990).
[17] B. Gall, H. Flocard, P.-H. Heenen, P. Bonche, and J. Dobaczewski, Z. Phys. A **348**, 183 (1994).
[18] E. F. Moore *et al.*, Phys. Rev. Lett. **63**, 360 (1989).
[19] M. P. Carpenter *et al.*, Phys. Lett. B **240**, 44 (1990).
[20] R. Bengtsson and S. Frauendorf, Nucl. Phys. **A327**, 139 (1979).
[21] J. A. Becker *et al.*, Phys. Rev. C **46**, 889 (1992).
[22] K. Thiene *et al.*, Z. Phys. A **336**, 113 (1990); M. J. Brinkman *et al.*, *ibid.* **336**, 115 (1990).
[23] M. J. Joyce *et al.*, Phys. Rev. Lett. **71**, 2176 (1993).